Characterizing Photochemical Transformation of Aqueous nC_{60} under Environmentally Relevant Conditions

YU SIK HWANG AND QILIN LI*

Department of Civil and Environmental Engineering, Rice University, Houston Texas 77005

Received December 7, 2009. Revised manuscript received March 11, 2010. Accepted March 17, 2010.

Engineered nanomaterials may undergo transformation upon interactions with various environmental factors. In this study, photochemical transformation of aqueous nC_{60} was investigated under UVA irradiation. nC_{60} underwent photochemical transformation in the presence of dissolved O_2, resulting in surface oxygenation and hydroxylation as demonstrated by XPS and ATR-FTIR analyses. The reaction followed a pseudo-first order rate law with the apparent reaction rate constant of 2.2×10^{-2} h^{-1}. However, the core of the nanoparticles remained intact over 21 days of irradiation. Although no mineralization or dissolution of nC_{60} was observed, experiments using fullerol as a reference fullerene derivative suggested likely dissolution and partial mineralization of nC_{60} under long-term UVA exposure. Aquatic humic acid reduced nC_{60} transformation kinetics presumably due to scavenging of reactive oxygen species. Results from this study imply that photochemical transformation is an important factor controlling nC_{60} physical and chemical properties as well as its fate and transport in the natural aqueous environment. In addition, changes in nC_{60} surface chemistry drastically reduced C_{60} extraction efficiency by toluene, suggesting that the existing analytical method for C_{60} may not be applicable to environmental samples.

Introduction

Because of the unique physical, chemical, and electronic properties attributable to their cage-like structures, fullerenes are proposed for use in a wide range of applications including optical, electronic, cosmetic, biomedical, and environmental applications (*1*−*3*). Although relevant environmental regulations are still in discussion, fullerene-based consumer products are already commercially available (*4*). It is now well recognized that the potential large scale production of nanomaterials such as fullerenes and their widespread use in consumer products will inevitably result in their appearance in natural environment. Concerns over the potential negative impacts on human health and ecosystems have motivated intensive study on the environmental fate and transport of nanomaterials.

C_{60} is one of the most attractive nanomaterials. Despite its extremely low water solubility, C_{60} forms stable nanosized particles in water, usually referred to as nC_{60}, through solvent exchange or extended stirring (*5*−*7*). nC_{60} nanoparticles are considered an environmentally relevant form of C_{60} and are being intensively studied regarding their formation, aggregation, transport, and toxicity (*8*−*14*). However, most existing studies on nC_{60} fate and transport were performed under simplified laboratory conditions, not representative of the actual natural environment. The physicochemical properties and chemical nature of nC_{60} can be altered by environmental factors such as natural organic matter and sunlight. Such environmental transformations will likely change its environmental fate and toxicity.

C_{60} possesses strong light absorptivity in the UV range and is known to be highly photosensitive in organic solvents (*15, 16*). However, little is known about photochemical transformation, a primary process for natural transformation of organic chemicals, of nC_{60} itself in water. Based upon the photochemical transformation or degradation of a wide variety of aromatic organic compounds (e.g., PAHs) (*17*−*19*), the photochemical transformation of fullerene is likely to be an important environmental transformation pathway, particularly in surface waters. Hou and Jafvert (*20, 21*) first reported decomposition of nC_{60} upon long-term exposure to sunlight. nC_{60} particles were found to disintegrate over time and soluble reaction products were formed. Meanwhile, singlet oxygen production was observed in the presence of dissolved oxygen. Another study found that sunlight greatly enhanced the dispersion of C_{60} into water and the nanoparticles dispersed under sunlight were photochemically modified (*22*). More recently, Lee et al. (*23*) analyzed the photochemical transformation products of nC_{60} after exposure to UVC (254 nm). Water-soluble compounds containing various oxygen functional groups were identified as the major products.

The objective of the reported study was to understand the photochemical transformations of nC_{60} that may occur in natural aqueous environments. nC_{60} suspensions were exposed to UVA irradiation (300−400 nm in wavelength), the main component of UV light in solar irradiation. Changes in physicochemical properties and chemical composition of nC_{60} were examined using various analytical techniques, including total organic carbon (TOC), dynamic light scattering (DLS), transmission electron microscopy (TEM), UV/vis spectroscopy, X-ray photoelectron spectroscopy (XPS), and Fourier transform infrared (FTIR) spectroscopy. The effect of humic acid on the photochemical transformation rate was also evaluated.

Materials and Methods

Chemicals. Sublimed C_{60} fullerene powder (99.9% purity) and hydroxylated C_{60}, fullerol ($C_{60}(OH)_x(ONa)_y$, $x+y = 24$, $y = 6-8$) were obtained from Materials Electronics Research Corporation (Tucson, AZ). Suwannee River humic acid (SRHA) standard (II) was purchased from International Humic Substances Society (IHSS, Atlanta, GA). The SRHA stock solution at 625 mg/L was prepared by dissolving SRHA powder in deionized water, adjusting the pH to 7.5 with NaOH, and filtering through a 0.45 μm pore size Whatman membrane filter. Toluene used was Omnisolv grade with over 99.99% assay (EMD Chemicals Inc., Gibbstown, NJ). Other chemicals were reagent grade with purity greater than 99% (Fisher Scientific, Fair Lawn, NJ). All aqueous samples were prepared using double deionized water produced by a Barnstead Epure system (Dubuque, IA).

nC_{60} Suspension Preparation. Aqueous nC_{60} suspensions were prepared using a direct sonication method without the use of an organic solvent. C_{60} powder was pulverized using agate mortar and pestle for 10 min to enhance the dispersion rate and consistency. An aliquot of 150 mg pulverized C_{60}

* Corresponding author phone: (713)348-2046; fax: (713)348-2026; e-mail: qilin.li@rice.edu.

10.1021/es903713j © XXXX American Chemical Society

was added to 200 mL of deionized water in a 500 mL glass beaker. The C_{60}-water mixture was then sonicated using a sonicating probe (Vibra-Cell VCX 500, Sonics & Material, Newtown, CT) operated at 20% intensity (100 W) for 30 min. The resulting suspension was then filtered through 2 μm pore size Millex-AP membrane filters to remove large aggregates. Several batches were prepared and combined to avoid batch to batch variation. The stock suspension was stored in dark at 4 °C. Particle size and C_{60} concentration were routinely monitored and were constant within the period of this study.

Irradiation Experiments. Irradiation experiments were performed in a Luzchem LZC-4V photoreactor (Luzchem, Ottawa, Ontario, Canada). The photoreactor was equipped with four 8 W black lamps (Hitachi FL8BL-B) that emit UVA in the wavelength range of 300−400 nm centered at 350 nm. UVA is the main component of UV light in the solar spectrum. It makes up 4−5% of the total solar irradiation. The light intensity at the center of the reactor was measured at approximately 2 mW/cm^2 using a Radiometer (Control Company, Friendswood, TX), comparable to the UVA intensity of sunlight at the ground level on a sunny summer day in Houston, Texas. In each experiment, four Erlenmeyer flasks each containing 50 mL of sample were placed on the merry-go-round at the center of the photoreactor and rotated to ensure uniform exposure. All suspensions contained 3.8 mg/L nC_{60} and 1 mM NaCl with unadjusted pH between 6 and 6.5. No detectable changes in pH were observed during experiments. For experiments with SRHA, the SRHA stock solution was added to nC_{60} samples to achieve desired concentrations. All samples were mixed for 30 min prior to irradiation. As the photochemical reaction proceeded, samples were withdrawn from the flasks for analysis. A ventilation system circulated ambient air through the reactor to maintain the temperature at 25 ± 2 °C. For experiments under anoxic conditions, the flasks were purged with ultrapure N_2 for 2 h before the experiment and sealed. N_2 purging was also maintained during sampling. All kinetic experiments were performed in triplicate.

Quantitative Analysis of C_{60}. nC_{60} concentration was determined using a liquid−liquid extraction method (*12*). Briefly, a portion of each sample, toluene, and 0.1 M $Mg(ClO_4)_2$ were combined in the ratio of 5:5:2 and vigorously mixed for 2 h on a orbital shaker. The extracted toluene phase was analyzed by atmospheric pressure photoionization (APPI) mass spectrometry to identify extracted compounds. The concentration of C_{60} extracted into toluene was then determined by measuring UV absorbance at 335 nm, based upon a calibration curve established using C_{60} solutions in toluene (molar absorption coefficient = 0.0754 L mg^{-1} cm^{-1}). Total organic carbon (TOC) concentration of nC_{60} samples was measured with a high sensitivity TOC analyzer (Shimadzu Scientific Instruments, Columbia, MD).

Particle Characterization. Particle size and electrophoretic mobility of nC_{60} particles were measured by dynamic light scattering (DLS) and phase analysis light scattering, respectively, using a Nano Zeta-sizer (Malvern Instruments, Worcestershire, UK). The morphology and size of the particles were also characterized using a JEOL-2010 transmission electron microscope (TEM) (JEOL Inc., Peabody, MA). Samples for TEM analysis were prepared by depositing 3 μL sample suspension on a 400-mesh carbon support film on copper grid (Ted Pella, Redding, CA) and drying the sample at room temperature overnight. UV/vis absorbance spectra were obtained using a dual beam, high resolution UV/vis spectrophotometer (UV-2550, Shimadzu Scientific Instruments, Columbia, MD).

For more detailed characterization, XPS and attenuated total reflectance (ATR)-FTIR analyses were performed with concentrated samples (~100 mg/L). A protein concentrating centrifugal cartridge with a molecular weight cutoff of 30 kDa (Amicon Ultra 15, Millipore) was used to concentrate the suspensions at 5000 rpm for 15 min. The XPS analysis was carried out using a PHI Quanteria SXM scanning X-ray microprobe ULVAC-PHI with an Al mono, 24.8 WX- ray source and a 200.0 μm X-ray spot size at 45.0° (26.00 eV). XPS samples were prepared by sputter coating a clean silicon wafer with Au for 2 min at 100 mA and then evaporating 150 μL of the concentrated samples on the wafer at room temperature overnight (*24*). The ATR-FTIR analysis was conducted using a Thermo Nicolet Nexus 670 FTIR spectrometer equipped with a NICOLET Smart Golden Gate accessory. Fullerol was also analyzed by XPS and FTIR as a reference compound of derivatized C_{60}. Fullerol suspensions were prepared by magnetically stirring the fullerol powder in deionized water for 24 h and filtering the suspension through 2 μm pore size Millex-AP membrane filters.

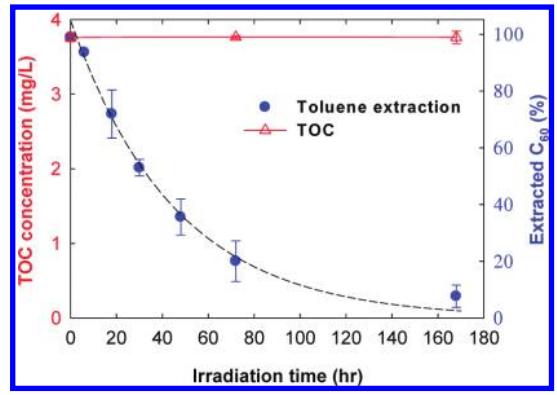

FIGURE 1. TOC and extracted C_{60} concentrations as a function of UV irradiation time.

Results and Discussion

Photochemical Transformation of nC_{60}. The extent of photochemical transformation was evaluated by measuring TOC and nC_{60} concentration using the toluene-$Mg(ClO_4)_2$ extraction procedure (Figure 1). APPI-MS analysis of the extracted toluene phase showed that C_{60} was the only compound extracted into toluene from the unirradiated and irradiated samples (Supporting Information (SI) Figure S1). It is noted that the concentration measured using the toluene-$Mg(ClO_4)_2$ extraction method does not represent the total concentration of C_{60} in the irradiated suspensions as explained later. Although recovery of C_{60} is close to 100% for underivatized nC_{60} (*12, 25*), changes in surface chemistry from photochemical transformation reactions may reduce the extraction efficiency. Therefore, the term "extracted C_{60}" instead of "C_{60} concentration" is used in describing the photochemical transformation rate. The reduction in the amount of C_{60} extracted includes the loss of C_{60} due to photochemical reactions as well as that due to reduction in toluene extraction efficiency.

The dark control samples showed no measurable loss in extracted C_{60} concentration (data not shown) over 3 months, suggesting that no chemical transformation occurred in dark. Upon UV irradiation, the extracted C_{60} concentration decreased rapidly with irradiation time with approximately 95% reduction after 7 days. These data show that nC_{60} underwent substantial photochemical transformation during the 7-day irradiation. Based on the loss in the extracted C_{60} concentration, the apparent transformation kinetics can be described by a pseudo-first order reaction with an reaction rate constant of 2.2×10^{-2} h^{-1}, corresponding to a half-life of 31 h. These values are similar to those reported by Hou and Jafvert using sunlight (*20*). On the other hand, TOC concentration remained unchanged, suggesting no carbon mineralization

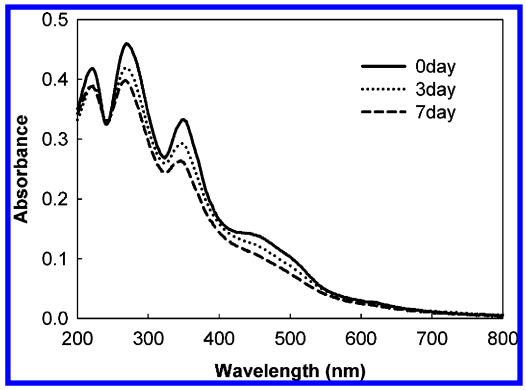

FIGURE 2. UV/vis spectra of nC_{60} at different irradiation time.

within this time frame. A very small decrease in TOC concentration (0.25 mg/L) was observed after 21 days of irradiation, much lower than that reported by Hou and Jafvert based on the sum of C_{60} concentration and soluble organic carbon (*20*). Two potential reasons exist for such discrepancy: Most phototransformation products are insoluble in water and remain on the particle surface (i.e., not accounted for by soluble organic carbon); The toluene-$Mg(ClO_4)_2$ extraction method underestimates C_{60} concentration when the surface of nC_{60} is derivatized due to phototransformation.

Characterization of Photochemical Transformation Product(s). Although significant photochemical transformation of nC_{60} was observed, there were no notable changes in physical properties of the nanoparticles within the 21-day irradiation time. The yellow color of solution faded slightly, while the particle size and surface zeta-potential remained fairly constant. TEM imaging did not show notable changes in particle morphology or size. Tables S1 and S2 summarize the physical properties of the nC_{60} suspension during the 21-day exposure. The unchanged particle size and morphology suggest negligible release of soluble phototransformation products from the particles.

Figure 2 illustrates changes in the UV/vis spectrum of nC_{60} during the 7-day irradiation. All absorbance spectra showed maxima at 270 and 350 nm, and a broad band between 410 and 555 nm, suggesting the presence of C_{60} in the form of aggregated clusters (*12*). The absorbance between 200 and 800 nm slowly decreased as irradiation time increased, although the extent of this decrease varied with wavelengths. For example, a 20% reduction in the absorbance at 350 nm, which is commonly used for nC_{60} concentration measurement, was observed after 7 days of irradiation, while the absorbance spectrum of the dark control remained unchanged. An excellent correlation between the UV absorbance at 350 nm and C_{60} concentration of the dark control samples was also obtained (SI Figure S2), indicating that the reduction in UV absorbance observed in the irradiation experiment could be attributed to a reduction in C_{60} concentration due to photochemical transformation of C_{60}, in agreement with the observation from nC_{60} concentration measurement by the toluene extraction method. Quantitatively, however, the reduction in UV absorbance at 350 nm (20%) was much lower than that in the extracted C_{60} (95%) after 7 days of irradiation. An increase in irradiation time from 7 to 21 days resulted in an additional 17% reduction in UV absorbance at 350 nm, while the extracted C_{60} concentration decreased from 5 to 3% of the initial concentration. Two factors potentially contribute to such discrepancy. Firstly, the intermediate product(s) of photochemical transformation absorbs light in the wavelength range of 200−800 nm and undergoes further transformation; secondly, the photochemical transformation reactions on the nC_{60} nanoparticle surface reduce the recovery of toluene extraction. The observed reduction in UV absorbance was also much

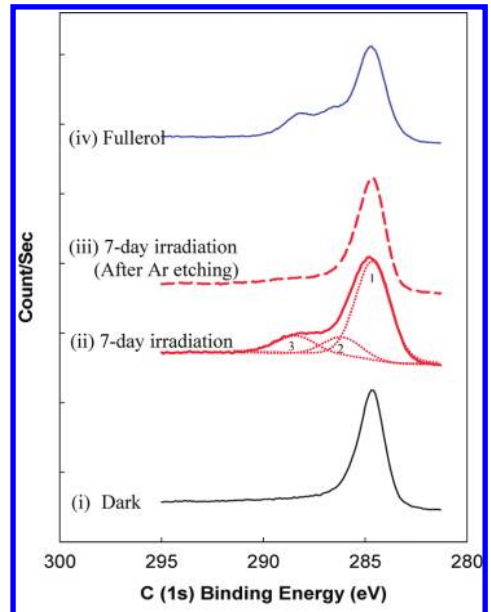

Peak	Position	% C(1s)	Carbon
1	284.3	66%	Underivatized C
2	285.6	19%	Mono-oxygenated C
3	288.0	15%	Di-oxygenated C

FIGURE 3. C(1s) XPS spectra of (i) nC_{60} dark control, (ii) nC_{60} after 7-day irradiation product, (iii) 7-day irradiated sample after Ar etching, and (iv) fullerol suspension. Dot line in (ii) spectrum represents curve fitting deconvolution.

slower than that reported by Lee et al. using UVC (254 nm), which showed ~20% reduction in the absorbance at 350 nm within 2−3 h (*23*). The difference is attributed to the higher absorptivity of C_{60} at 254 nm and the higher intensity of irradiation used in that study.

In order to examine the changes in chemical composition of nC_{60} nanoparticles as a result of photochemical transformation, XPS analysis was performed. Figure 3 compares the binding energy spectra of C(1s) electrons in the dark control (spectrum i) and the sample after 7 days of irradiation (spectrum ii). The XPS spectra of both samples have one C(1s) peak at 284.3 eV, which can be attributed to sp2 hybridized carbon in C_{60}. For the irradiated sample, however, a broad shoulder at higher binding energies was observed, indicating the presence of highly oxidized carbon. Spectral deconvolution suggests the presence of mono-oxygenated carbon (C—O) at 285.6 eV and dioxygenated carbon (C═O or O—C—O) at 288 eV at 19 and 15%, respectively, of the total carbon. These functionalities are the same as those reported by Lee et al. (*23*) for nC_{60} suspensions irradiated by UVC at 254 nm. In addition, the XPS spectrum of the irradiated sample was similar to that of fullerol, a reference fullerene derivative, (spectrum iv, Figure 3), indicating the similarity in surface chemistry to fullerol.

It should be noted that XPS only probes the outer surface of the particles with a penetration depth of 3−5 nm. In order to determine whether the photochemical transformation occurred throughout the nC_{60} particles, the core of the particles was further analyzed by XPS after 1 min of Argon ion etching (3 kV) to a depth of approximately 3 nm from the particle surface. After the etching, the two peaks at higher energy levels disappeared (spectrum iii, Figure 3). In contrast, the spectrum of the fullerol sample remained essentially unchanged after the same etching process (SI Figure S3). This suggests that oxidation of nC_{60} during the 7-day irradiation occurred only on the outer surface of the nanoparticles. The core of the nanoparticles was still un-

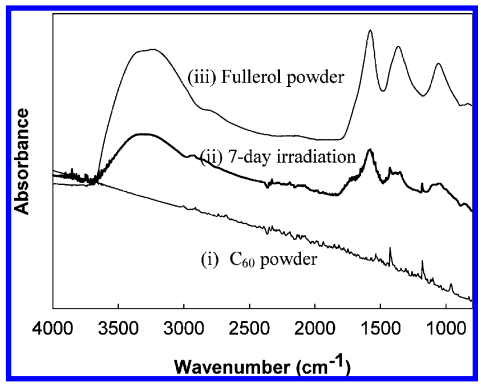

FIGURE 4. ATR-FTIR spectra of (i) C_{60} powder, (ii) nC_{60} after 7-day irradiation, and (iii) fullerol powder.

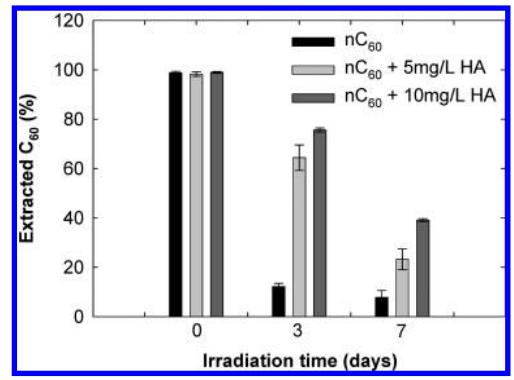

FIGURE 5. Effect of Suwannee River humic acid on photochemical transformation of nC_{60}.

derivatized C_{60}. This is consistent with the small changes of UV/vis absorbance shown in Figure 2, supporting our hypothesis that photochemical transformation on nC_{60} surface reduces toluene extraction efficiency and the C_{60} concentration determined by the toluene extraction method overestimates the photochemical reaction rate. Since there was no change in particle size and morphology during the same period, this result also indicates that the photochemical oxidation products on the particle surface were not soluble in water and hence not released from the particles. This differs from the finding of Hou and Jafvert (*20*) and Lee et al. (*23*) that nC_{60} particle size decreased with irradiation time. This may be attributed to the difference in reaction kinetics due to different irradiation intensity and time as well as nC_{60} preparation method and hence nC_{60} particle properties.

ATR-FTIR characterization of nC_{60} suspensions after irradiation provides further evidence for photochemical oxidation of nC_{60} particle surface (Figure 4). The IR spectrum of pristine C_{60} showed two sharp peaks at 1180 and 1430 cm^{-1}, attributed to the C−C vibration of C_{60} (spectrum i). The IR spectrum of the reference fullerol (spectrum iii) exhibited several broad peaks at 3400 cm^{-1} (O−H), 1710 cm^{-1} (C=O), 1590 cm^{-1} (C=C), 1370 cm^{-1} (C=C or C−O−H), and 1060 cm^{-1} (C−O). These spectra are consistent with previously reported data for C_{60} powder as well as nC_{60} (*26, 27*) and fullerols (*28, 29*). Similar to that observed in XPS analysis, the IR spectrum of the irradiated sample (spectrum ii) showed the same absorbance peaks as those of fullerol. These same absorbance peaks were reported for C_{60} oxidized by ozone (*24*) or upon UVC irradiation (*23*). Unlike these previous studies, however, two sharp peaks at 1180 and 1430 cm^{-1} corresponding to the parent C_{60} vibrations were also observed in the spectrum of the product. This confirms that the core of the particles is still underivatized C_{60}.

Role of Dissolved Oxygen. The oxidative nature of the photochemical transformation process suggests the involvement of an oxidant, e.g., dissolved oxygen in water. Irradiation experiments under anoxic conditions found that nC_{60} transformation was negligible in the absence of oxygen, in contrast to the rapid decrease in extracted C_{60} concentration in the presence of dissolved oxygen (SI Figure S4). This is consistent with previous studies using both UVA and UVC irradiation (*20, 23*).

Effect of NOM on Photochemical Transformation Kinetics. Natural organic matter (NOM) is ubiquitous in the aqueous environment. nC_{60} in the aqueous environment will inevitably encounter NOM, which is known to readily adsorb onto nC_{60} surface (*25, 30*). To examine the effect of NOM on nC_{60} photochemical transformation, irradiation experiments were also performed in the presence of SRHA as a model NOM. Results are presented in Figure 5. Without irradiation, the toluene-$Mg(ClO_4)_2$ extraction method was able to recover 97−99% of C_{60} from the nC_{60} suspension in the presence of SRHA, suggesting that nC_{60} was chemically intact in the presence of SRHA and SRHA did not interfere with toluene extraction of C_{60}. However, the presence of SRHA significantly reduced the photochemical transformation rate of nC_{60}, as demonstrated by the higher extracted C_{60} concentration compared to that in the absence of SRHA. This inhibitive effect was more profound at higher SRHA concentrations. After 7 days of irradiation, the extracted C_{60} was 7, 24, and 40% of the initial concentration with 0, 5, and 10 mg/L SRHA, respectively. NOM is known to generate reactive oxygen species (ROS) upon photosensitization (*31, 32*). There have been many studies demonstrating enhanced photodegradation of organic chemicals in the presence of NOM due to NOM mediated ROS formation (*19, 33*). On the other hand, NOM can also reduce photodegradation rate through both light screening and ROS scavenging (*19, 34*). In our study, the observed inhibitive effect of NOM on nC_{60} transformation suggests that NOM mediated photochemical transformation was not an important pathway. Instead, light screening and scavenging of ROS by humic acid adsorbed on nC_{60} surface are more prominent mechanisms.

Photochemical Transformation of Fullerol. Because of the similarity between the surface of phototransformed nC_{60} and fullerol as demonstrated in the XPS and ATR-FTIR results, fullerol was used as a reference compound for the intermediate phototransformation products formed on nC_{60} surface. Additional experiments using fullerol were carried out to indirectly investigate the long-term photochemical fate of nC_{60}. The initial TOC concentration of the fullerol samples was kept the same as that of nC_{60} suspensions used in experiments described above (i.e., 3.8 mg C/L). Figure 6a presents the changes in the UV/vis spectrum of the fullerol suspension during 21 days of irradiation. Unlike nC_{60}, the fullerol suspension does not have any absorbance maximum in the wavelength range of 200−800 nm. However, it does exhibit significant UV absorbance in this wavelength range. The reaction products are expected to have a lower level of oxygenation or hydroxylation than fullerol and hence UV/vis absorbance between that of nC_{60} and fullerol. This suggests that the UV absorbance of the irradiated nC_{60} (Figure 2) is partly attributable to photochemical oxidation products on nC_{60} surface. Therefore, direct measurement of UV absorbance may overestimate C_{60} concentration. With irradiation, the UV/vis absorbance of the fullerol solution decreased with time, indicating decreased π-conjugation presumably due to increased hydroxylation or oxygenation of the sp2 carbons, which has been shown to lighten the color of aqueous fullerol solutions (*35*). The originally yellow color solution became almost colorless after 21 days of irradiation.

Reduction in TOC was observed during irradiation of the fullerol solution, showing mineralization of fullerol due to photochemical oxidation. Changes in UV absorbance (at 350 nm) and TOC concentration of fullerol as a function of irradiation time are presented in Figure 6b. Both the UV

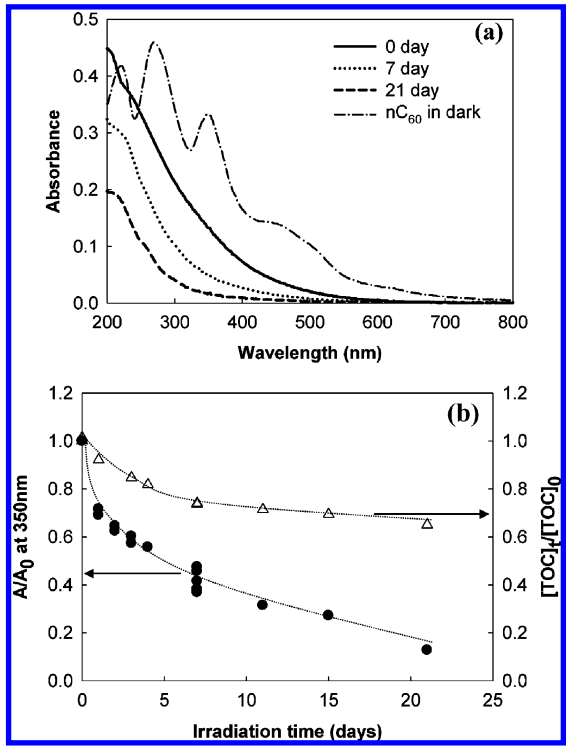

FIGURE 6. Changes of a fullerol suspension due to photochemical transformation. The initial TOC concentration was 3.8 mg C/L. (a) UV/vis spectra of fullerol at different UV irradiation time and the nC_{60} dark control. (b) Absorbance at 350 nm (left axis) and TOC (right axis) of fullerol as a function of UV irradiation time.

absorbance and TOC in the first week of irradiation could be described by a pseudo-first order reaction with rate constants of 4.6×10^{-3} h^{-1} ($R^2 = 0.90$) and 1.8×10^{-3} h^{-1} ($R^2 = 0.97$), respectively. The greater reduction in UV/vis absorbance (58% in absorbance at 350 nm after 7 days) and the substantial loss in TOC of the fullerol suspension compared to the nC_{60} suspension indicate that fullerol is more susceptible to photochemical transformation. After 7 days of irradiation, the UV/vis absorbance continued to decrease following the pseudo-first order reaction kinetics, whereas the TOC concentration appeared to reach a plateau. From the data shown in Figure 6, it is estimated that approximately 60% of the initial TOC will remain as non UV-absorbing compounds. These results are consistent with the study by Kong et al. (*36*), which reported 47% mineralization of fullerol during simulated solar irradiation .

Photochemical Transformation of nC_{60} and Its Environmental Implication. Our study showed that photochemical transformation of nC_{60} occurred at significant rates under UVA irradiation at intensity similar to sunlight in the presence of oxygen. The nC_{60} surface was oxygenated/hydroxylated, resulting in intermediate products similar to fullerol. Unlike that observed with UVC irradiation (*23*), no significant release of soluble reaction products was observed within 3 weeks of irradiation. The photochemical oxidation reaction was limited to the surface of the nC_{60} nanoparticles for an extended period of time (e.g., 21 days) with the particle core unchanged. Changes in particle surface chemistry led to decrease in C_{60} extraction efficiency by the toluene-$Mg(ClO_4)_2$ method, suggesting that the existing analytical method for C_{60} may not be applicable to environmental samples in which nC_{60} particle surface is altered by phototransformation. These changes are expected to alter nC_{60} transport behaviors including aggregation and deposition as well as bioavailability and toxicity. Therefore, photochemical transformation processes should be considered carefully in environmental fate and transport modeling and risk assessment of C_{60}. Experiments with fullerol as a hydroxylated intermediate reaction product demonstrated the potential of mineralization of C_{60} over long-term irradiation, although a large fraction of transformation products remained as non-UV absorbing soluble compounds, whose chemical nature and environmental impact are unknown. In addition, photochemical transformation of fullerol may limit its potential application as a photocatalyst for water treatment (*37, 38*).

Acknowledgments

This work was supported by the NSF Center for Biological and Environmental Nanotechnology (Award EEC-0647452) and the USEPA STAR program (Grant No. 834093). We thank Drs. Bo Chen and Wenhua Guo and Seung Soo Lee at Rice University for their assistance in XPS and TEM analyses. We also thank Dr. William Hockaday at Rice University for assistance in APPI-MS analysis.

Supporting Information Available

Figures illustrating APPI-MS analysis of the extracted toluene phase, UV/vis spectra of nC_{60} as a function of concentration, XPS spectrum of fullerol sample after Ar etching, and effect of O_2 on nC_{60} photochemical transformation kinetics, and tables showing physical properties of nC_{60} before and after UVA irradiation are provided. This material is available free of charge via the Internet at http://pubs.acs.org.

Literature Cited

(1) Murayama, H.; S., T.; Michael, A. J.; E., K. M. Fullerene production in tons and more: From science to industry. *Fullerenes, Nanotubes, Carbon Nanostruct.* **2004**, *12*, 1–9.
(2) Mauter, M. S.; Elimelech, M. Environmental applications of carbon-based nanomaterials. *Environ. Sci. Technol.* **2008**, *42*, 5843–5859.
(3) Osawa, E., *Perspective of Fullerene Nanotechnology*: Springer: Berlin, Germany, 2002.
(4) Nanotechnology consumer products inventory. http://www.nanotechproject.org/inventories/consumer/ (Accessed November 1, 2009).
(5) Andrievsky, G. V.; Kosevich, M. V.; Vovk, O. M.; Shelkovsky, V. S.; Vashchenko, L. A. On the production of an aqueous colloidal solution of fullerenes. *J. Chem. Soc. Chem. Commun.* **1995**, *12*, 1281–1282.
(6) Deguchi, S.; Alargova, R. G.; Tsujii, K. Stable dispersions of fullerenes, C_{60} and C_{70} in water. Preparation and characterization. *Langmuir* **2001**, *17*, 6013–6017.
(7) Cheng, X.; Kan, A. T.; Tomson, M. B. Naphthalene adsorption and desorption from aqueous C_{60} fullerene. *J. Chem. Eng. Data* **2004**, *49*, 675–683.
(8) Brant, J. A.; Labille, J.; Bottero, J. Y.; Wiesner, M. R. Characterizing the impact of preparation method on fullerene cluster structure and chemistry. *Langmuir* **2006**, *22*, 3878–3885.
(9) Chen, K. L.; Elimelech, M. Aggregation and deposition kinetics of fullerene (C_{60}) nanoparticles. *Langmuir* **2006**, *22*, 10994–11001.
(10) Dhawan, A.; Taurozzi, J. S.; Pandey, A. K.; Shan, W.; Miller, S. M.; Hashsham, S. A.; Tarabara, V. V. Stable colloidal dispersion of C_{60} fullerenes in water: Evidence for genotoxicity. *Environ. Sci. Technol.* **2006**, *40*, 7394–7401.
(11) Duncan, L. K.; Jinschek, J. R.; Vikesland, P. J. C_{60} colloid formation in aqueous systems: Effects of preparation method on size, structure, and surface, charge. *Environ. Sci. Technol.* **2008**, *42*, 173–178.
(12) Fortner, J. D.; Lyon, D. Y.; Sayes, C. M.; Boyd, A. M.; Falkner, J. C.; Hotze, E. M.; Alemany, L. B.; Tao, Y. J.; Guo, W.; Ausman, K. D.; Colvin, V. L.; Hughes, J. B. C_{60} in water: Nanocrystal formation and microbial response. *Environ. Sci. Technol.* **2005**, *39*, 4307–4316.
(13) Sayes, C. M.; Fortner, J. D.; Guo, W.; Lyon, D.; Boyd, A. M.; Ausman, K. D.; Tao, Y. J.; Sitharaman, B.; Wilson, L. J.; Hughes, J. B.; West, J. L.; Colvin, V. L. The differential cytotoxicity of water-soluble fullerenes. *Nano Lett.* **2004**, *4*, 1881–1887.

(14) Lyon, D. Y.; Adams, L. K.; Falkner, J. C.; Alvarez, P. J. J. Antibacterial activity of fullerene water suspensions: effects of preparation method and particle size. *Environ. Sci. Technol.* **2006**, *40*, 4360–4366.
(15) Taylor, R.; Parsons, J. P.; Avent, A. G.; Rannard, S. P.; Dennis, T. J.; Hare, J. P.; Kroto, H. W.; Walton, D. R. M. Degradation of C_{60} by light. *Nature* **1991**, *351*, 277–277.
(16) Creegan, K. M.; Robbins, J. L.; Robbins, W. K.; Millar, J. M.; Sherwood, R. D.; Tindall, P. J.; Cox, D. M.; Smith, A. B.; McCauley, J. P.; Jones, D. R.; Gallagher, R. T. Synthesis and characterization of $(C_{60})O$, the 1st fullerene epoxide. *J. Am. Chem. Soc.* **1992**, *114*, 1103–1105.
(17) Fasnacht, M. P.; Blough, N. V. Aqueous photodegradation of polycyclic aromatic hydrocarbons. *Environ. Sci. Technol.* **2002**, *36*, 4364–4369.
(18) Fasnacht, M. P.; Blough, N. V. Mechanisms of the aqueous photodegradation of polycyclic aromatic hydrocarbons. *Environ. Sci. Technol.* **2003**, *37*, 5767–5772.
(19) Jacobs, L. E.; Weavers, L. K.; Chin, Y. P. Direct and indirect photolysis of polycyclic aromatic hydrocarbons in nitrate-rich surface waters. *Environ. Toxicol. Chem.* **2008**, *27*, 1643–1648.
(20) Hou, W. C.; Jafvert, C. T. Photochemical transformation of aqueous C_{60} clusters in sunlight. *Environ. Sci. Technol.* **2009**, *43*, 362–367.
(21) Hou, W. C.; Jafvert, C. T. Photochemistry of aqueous C_{60} clusters: Evidence of $1O_2$ formation and its role in mediating C_{60} phototransformation. *Environ. Sci. Technol.* **2009**, *43*, 5257–5262.
(22) Li, Q.; Xie, B.; Hwang, Y. S.; Xu, Y. J. Kinetics of C_{60} fullerene dispersion in water enhanced by natural organic matter and sunlight. *Environ. Sci. Technol.* **2009**, *43*, 3574–3579.
(23) Lee, J.; Cho, M.; Fortner, J. D.; Hughes, J. B.; Kim, J. H. Transformation of aggregate C_{60} in the aqueous phase by UV irradiation. *Environ. Sci. Technol.* **2009**, *43*, 4878–4883.
(24) Fortner, J. D.; Kim, D. I.; Boyd, A. M.; Falkner, J. C.; Moran, S.; Colvin, V. L.; Hughes, J. B.; Kim, J. H. Reaction of water-stable C_{60} aggregates with ozone. *Environ. Sci. Technol.* **2007**, *41*, 7497–7502.
(25) Xie, B.; Xu, Z. H.; Guo, W. H.; Li, Q. Impact of natural organic matter on the physicochemical properties of aqueous C_{60} nanoparticles. *Environ. Sci. Technol.* **2008**, *42*, 2853–2859.
(26) Scharff, P.; Risch, K.; Carta-Abelmann, L.; Dmytruk, I. M.; Bilyi, M. M.; Golub, O. A.; Khavryuchenko, A. V.; Buzaneva, E. V.; Aksenov, V. L.; Avdeev, M. V.; Prylutskyy, Y. I.; Durov, S. S. Structure of C_{60} fullerene in water: spectroscopic data. *Carbon* **2004**, *42*, 1203–1206.
(27) Kratschmer, W.; Lamb, L. D.; Fostiropoulos, K.; Huffman, D. R. Solid C_{60} - a new form of carbon. *Nature* **1990**, *347*, 354–358.
(28) Xing, G. M.; Zhang, J.; Zhao, Y. L.; Tang, J.; Zhang, B.; Gao, X. F.; Yuan, H.; Qu, L.; Cao, W. B.; Chai, Z. F.; Ibrahim, K.; Su, R. Influences of structural properties on stability of fullerenols. *J. Phys. Chem. B* **2004**, *108*, 11473–11479.
(29) Schreiner, K. M.; Filley, T. R.; Blanchette, R. A.; Bowen, B. B.; Bolskar, R. D.; Hockaday, W. C.; Masiello, C. A.; Raebiger, J. W. White-rot basidiomycete-mediated decomposition of C_{60} fullerol. *Environ. Sci. Technol.* **2009**, *43*, 3162–3168.
(30) Chen, K. L.; Elimelech, M. Influence of humic acid on the aggregation kinetics of fullerene (C_{60}) nanoparticles in monovalent and divalent electrolyte solutions. *J. Colloid Interface Sci.* **2007**, *309*, 126–134.
(31) Schwarzenbach, R. P.; Gschwend, P. M.; Imboden, D. M., *Environmental Organic Chemistry*, 2nd ed.; John Wiley & Sons, Inc.: Hoboken, NJ, 2003.
(32) Stumm, W.; Morgan, J. J., *Aquatic Chemistry*, 3rd ed.; John Wiley & Sons, Inc.: New York, 1996.
(33) Zepp, R. G.; Baughman, G. L.; Schlotzhauer, P. F. Comparison of photochemical behavior of various humic substances in water 0.1. Sunlight induced reactions of aquatic pollutants photosensitized by humic substances. *Chemosphere* **1981**, *10*, 109–117.
(34) Walse, S. S.; Morgan, S. L.; Kong, L.; Ferry, J. L. Role of dissolved organic matter, nitrate, and bicarbonate in the photolysis of aqueous fipronil. *Environ. Sci. Technol.* **2004**, *38*, 3908–3915.
(35) Kokubo, K.; Matsubayashi, K.; Tategaki, H.; Takada, H.; Oshima, T. Facile synthesis of highly water-soluble fullerenes more than half-covered by hydroxyl groups. *ACS Nano* **2008**, *2*, 327–333.
(36) Kong, L.; Tedrow, O. N.; Chan, Y. F. K.; Zepp, R. G. Light-initiated transformations of fullerenol in aqueous media. *Environ. Sci. Technol.* **2009**, *43*, 9155−9160.
(37) Badireddy, A. R.; Hotze, E. M.; Chellam, S.; Alvarez, P.; Wiesner, M. R. Inactivation of bacteriophages via photosensitization of fullerol nanoparticles. *Environ. Sci. Technol.* **2007**, *41*, 6627–6632.
(38) Chae, S. R.; Hotze, E. M.; Wiesner, M. R. Evaluation of the oxidation of organic compounds by aqueous suspensions of photosensitized hydroxylated C_{60} fullerene aggregates. *Environ. Sci. Technol.* **2009**, *43*, 6208–6213.

ES903713J